RSC Advances

ROYAL SOCIETY OF CHEMISTRY

www.rsc.org/advances

Graphical Abstract

Anti-HSV activity and mode of action study

of α-pyrone carboxamides

Srinivas Karampuri, Durbadal Ojha, Paromita Bag, Harapriya Chakravarty, Chandralata Bal, Debprasad Chattopadhyay Ashoke Sharon

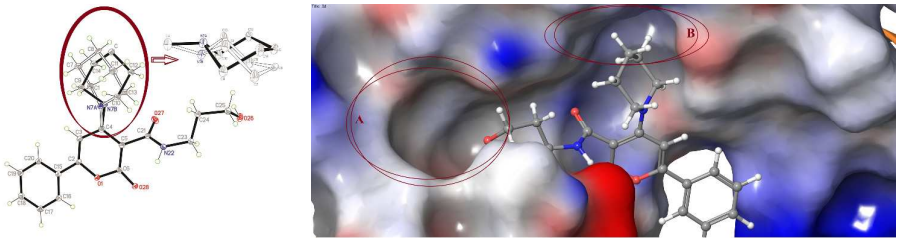

Potential anti-HSV lead candidate **3d** (EC_{50} = 9.8 μg/ml) and its possible binding mode to utilize cavity-A and cavity-B of viral enzyme HSV polymerase.

Anti-HSV activity and mode of action study of α-pyrone carboxamides

Srinivas Karampuri,[1,#] Durbadal Ojha,[2,#] Paromita Bag,[2] Harapriya Chakravarty,[1] Chandralata Bal,[1] Debprasad Chattopadhyay[2,*] Ashoke Sharon[1,*]

[1]*Department of Applied Chemistry, Birla Institute of Technology, Mesra, Ranchi 835215, India*

[2]*ICMR Virus Unit, ID & BG Hospital, Beliaghata, Kolkata 700010, India*

# These author contributed equally.

Address correspondence to:

Dr. Ashoke Sharon, Department of Applied Chemistry, Birla Institute of Technology, Mesra, Ranchi-835215, India Email: asharon@bitmesra.ac.in Phone: +91-651-2276531 Fax: +91-651-2275401

Dr. Debprasad Chattopadhyay, Scientist E, ICMR Virus Unit, ID & BG Hospital, Beliaghata, Kolkata 700010, India. Phone: +91-33-2353-7425; Telefax: +91-33-2353-7424
Email: debprasadc@yahoo.co.in

Abstract

The clinical management of herpes virus diseases is limited due to ineffective clearance of virus particles and frequent emergence of drug-resistant viruses, particularly in immunocompromised patients, pregnant women and neonates. In our continued quest for new antiviral lead, α-pyrone carboxamide propanol derivatives were synthesized and evaluated in HSV infected Vero cells. The compound **3d** showed potent antiviral activity against HSV-IF (EC_{50} = 9.8 μg/ml and EC_{99} = 18.0 μg/ml) and HSV-2G (EC_{50} = 12.4 μg/ml and EC_{99} = 24.0 μg/ml) at 4-6 h post-infection. The mode of action studies demonstrated that **3d** did not interfere in viral attachment or penetration, however, reduced the expression of ICP4 and ICP27 (immediate-early gene products) as well as the HSV DNA polymerase.

1. Introduction

The *Herpesviridae* are a large family of DNA viruses that include Herpes Simplex Virus type 1 and type 2 (HSV-1 and HSV-2). HSV-1 and HSV-2 are responsible for the cold sores and genital herpes that have plagued humanity for centuries. The DNA polymerase is one of the most important early proteins that play a key role during replication of these viruses. The HSV and human DNA polymerase belong to the family of type B DNA polymerase and share six to seven highly conserved domains including domain C.[1] We are focused to discover new non-nucleoside analogs (NNA) capable of doing selective inhibition of viral DNA polymerase. This may lead to achieve desirable inhibition with lesser side effects and toxicity. PNU-183792 **(I, Figure 1)** having broad spectrum anti-HSV activity with high specificity for viral polymerases compared to human polymerases is a 4-oxo-dihydroquinoline-3-carboxamide (DHQ) based derivative.[2] The earlier report shown that DHQ molecules were active in plaque reduction assays against various isolates of HSV and the average IC_{50}s were found in the range of 14 ± 4.0 µM in comparison to reference drug acyclovir (ACV) of 8.6 ± 5.4 µM.[2] Further, the studies on promising analog **I** shown comparable drug like properties with respect to licensed drugs acyclovir, ganciclovir, and cidofovir.[3]

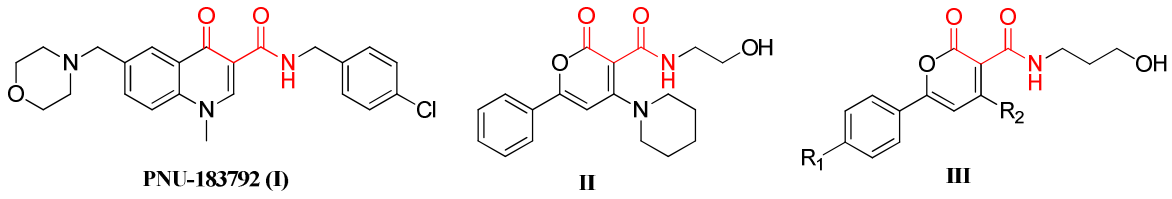

Figure 1 Chemical structure of potential compound PNU-183792 (**I**), preliminary lead (**II**) and new prototype molecules (**III**).

ACV, a synthetic guanine nucleoside analog is a prodrug that phosphorylates to ACV monophosphate preferentially by thymidine kinase of herpes virus, which then further phosphorylated to the di and tri-phosphate forms by cellular enzymes. The pharmacologically active ACV-triphosphate then inhibits the viral DNA polymerase along with chain termination. Despite the availability of ACV and its analogues the HSV can cause life-threatening infections such as herpes encephalitis. Neither acyclovir nor its analogues can eliminate the virus in the latent state[4]; while their extensive clinical use leads to the

emergence of drug-resistant viruses[5]. Consequently, continuation of the HSV pandemic is anticipated and efforts to develop vaccines and novel therapies aimed at eliminating latent virus are still warranted.[6,7] However, a recent study showed that anti-HSV therapy significantly reduces HIV-1 RNA load in co-infected patients.[8] Therefore, alternative treatments to minimize the development of resistance, its side-effects with better efficacy are urgently needed. Till date no antiviral compound has been able to completely inhibit the replication of any virus and a proportion of viral particles always seem to be able to circumvent the drug-induced blockade.

In our recent report, we described inclusion of pharmacophoric motif (red) of **I** for designing new molecules based on α-pyrone carboxamide and identified **II** (**Figure 1**) as our preliminary lead candidate with EC_{50} of 12.4 µg/ml and CC_{50} of 52.4 µg/ml.[9] The identification of pharmcophric motif were further followed by modeling studies and the preliminary lead compound **(II)** showed the possibility to fit into the allosteric site in palm region of HSV DNA polymerase. In addition, the two cavities were identified in the allosteric active site of polymerase, which were utilizing by piperdine and alcoholic mofit of **II**. Thus, to explore the possibility of our hypothesis, we extended our synthesis in this direction, so that target compounds can utilize these cavities more significantly to enhance anti-HSV activity. Therefore, new analogs (**III**, **Figure 1**) were selected with one more carbon (alcoholic motif) for synthesis, which may allow the molecule to utilize the remaining space of identified cavity to enhance anti-HSV activity. We had also carried out the modeling studies of **III** on understanding the molecular basis of compound binding in the allosteric site of viral DNA polymerase. If allosteric binding phenomenon exists, it opens a scope to evaluate the synergistic role of this compound (nonnucleoside inhibitor) with nucleoside inhibitor acyclovir. Thus, the mode of action studies including possible synergism was also carried out for one of the molecules with licensed drug ACV to test our hypothesis.

2. Results and Discussion

2.1 Synthesis of α-pyrone carboxamide derivatives

The α-pyrone-3-carboxylic acid derivatives (**1a-c**) were synthesized from appropriate acetophenone derivatives (**Scheme 1**).[9] The carboxyl group of **1a-c** was coupled with propanolamine using HATU as the coupling reagent to generate respective amides (**2a-c**).

The methylthio group at C-4 of **2a-c** was replaced with secondary amines by heating in dioxane to yield **3a-i**.

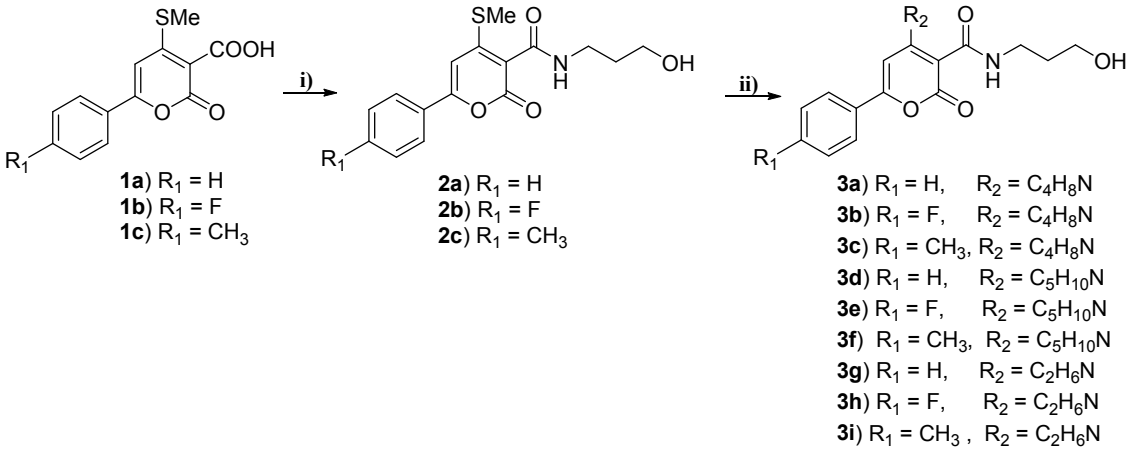

Scheme 1 Reagents and conditions: i) propanolamine, HATU, DMF, rt, 6h ii) appropriate amine, dioxane, 70ºC, 4h.

All the intermediates and final compounds were adequately characterized by spectroscopic analysis, and one of the potential lead compounds **3d** was further confirmed by a single crystal X-ray analysis.[10]

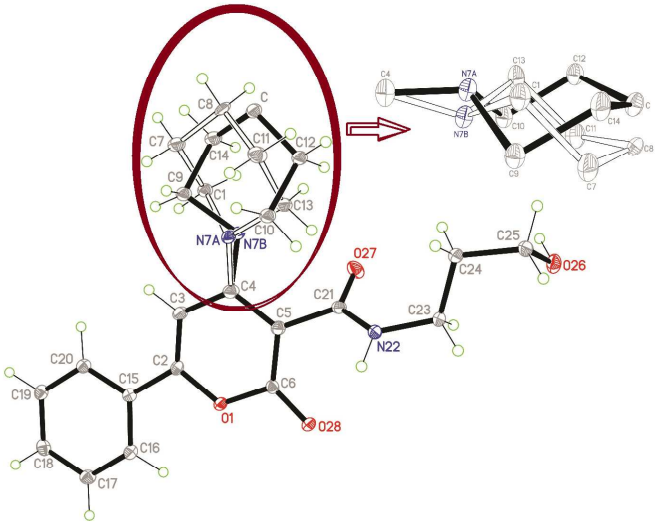

Figure 2. ORTEP diagram of **3d** showing the X-ray molecular structure in 30% probability level. The piperidine motif at C4 was found disordered due to conformational flipping in chair form of piperidine in the crystal structure. (CCDC # 970219)

The ellipsoidal plot as ORTEP diagram was shown with 30 % probability in Figure 2. The piperidine motif was found disordered, seen by two position of N7 atom at N7A and N7B and it may be

associated due to conformational flipping in chair conformation of piperidine ring. The complete X-ray structure was solved and refined with good resolution.

2.2 Biological Evaluation

2.2.1 Assessments of cytotoxicity and anti-HSV efficacy

The antiviral effects of **3a-i** were evaluated and results are presented in **Table 1**. Surprisingly out of nine only three compounds **(3a, 3d** and **3g)** showed anti-HSV activity below their CC_{50} concentrations. Compounds **3a** and **3g** were considered inactive as their EC_{50} values were above 30 µg/ml while **3d** with EC_{50} of 9.8 µg/ml was considered active. The only difference between the preliminary lead **(II, Figure 1)** and **3d** is in the hydroxyalkyl side chain and they seem to be structurally very close. Although, the anti-HSV activity (EC_{50}) was not improved much, the cytotoxicity of **3d** (CC_{50} = 151.4 µg/ml) has improved almost three times in comparison to **II** (CC_{50} = 52.4 µg/ml).[9] As a result the selectivity index (SI) of **3d** (15.4), which is a measure of the preferential antiviral activity of a drug in relation to its cytotoxicity (CC_{50}/EC_{50}) was also enhanced.

Table 1 Evaluation of Cytotoxicity and Anti-HSV activity of **3a-i**

Compound	CC_{50}[a] (µg/ml)	EC_{50}[b] (µg/ml)		SI (CC_{50}/EC_{50})[c]		EC_{99} (µg/ml)	
		HSV-1F	HSV-2G	HSV-1F	HSV-2G	HSV-1F	HSV-2G
II	52.4	12.4	13.1	4.23	4.0	22	28
3a	92.5	37.2	46.2	2.49	2.0	40	42
3b	39.4	36.4	>39	1.08	ND	>39	>39
3c	98.2	95	>98	1.03	ND	>98	>98
3d	**151.4**	**9.8**	**12.4**	**15.4**	**12.2**	**18**	**24**
3e	29.2	12	15	2.43	1.94	20	25
3f	43.6	40	>43	1.09	ND	>40	>40
3g	76.8	33.1	72	2.32	1.07	40	>72
3h	117.5	112.5	>117	1.04	ND	115	>117
3i	37.8	36.5	>37	1.03	ND	>37	>37
Acyclovir	**136.8**	**2.4**	**2.8**	**57.0**	**48.8**	**5.0**	**6.2**

[a]The 50% cytotoxic concentration for Vero cells (CCL 81) in µg/ml.
[b]Concentration of compound (µg/ml) producing 50% inhibition of virus induced CPE of three separate experiments.
[c]Selectivity index (SI) = CC_{50}/EC_{50} [SI Index below 4 is insignificant]
ND, Not detected, as the anti-HSV activity was either equal to or above the CC_{50} concentrations. The EC_{99} was above their CC_{50} concentrations, for most of the compounds.

2.2.2 Dose response assay

Vero cells were infected with HSV-1F or HSV-2G and exposed to the various concentrations of **3d** and acyclovir. The dose-dependent antiviral activity was evaluated by MTT assay. The results (**Figure 3**) revealed that **3d** inhibited HSV-1 and HSV-2 in a dose-dependent manner and maximum (> 99%) inhibition was observed at 18 and 24 µg/ml respectively. Acyclovir achieved > 99% inhibition at 5 µg/ml for both HSV-1 and HSV-2.

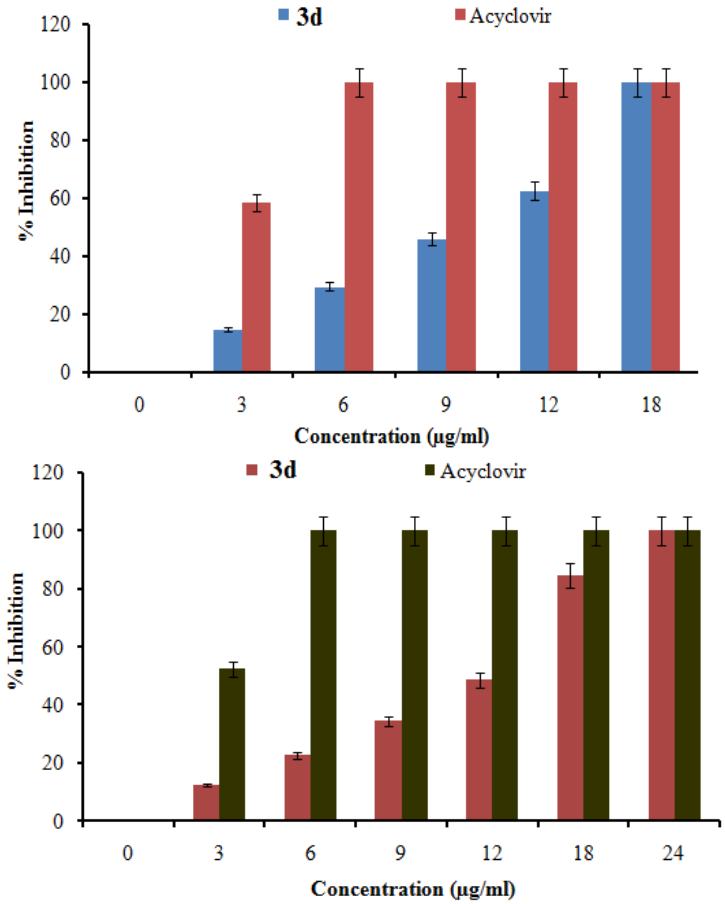

Figure 3 Dose dependent effects of **3d** and acyclovir against HSV-1F and HSV-2G. No inhibition was noticed with 0.1% DMSO, used as solvent (data not shown).

2.2.3 Time response assay

To investigate the activity of **3d** on viral infection cycle, we performed the time-of-addition assay. Addition of **3d** (18 µg/ml) to HSV-1F infected Vero cells at different time points revealed that it was effective at 4-6 h post-infection (hpi). No inhibition was found when the virus particles were exposed to **3d** before infection (pre-infection) or at the time of infection (co-infection). These findings suggested that the antiviral activity of **3d** was not due to the

inhibition of viral adsorption but due to the inhibition or blocking of early replication of HSV (**Figure 4**).

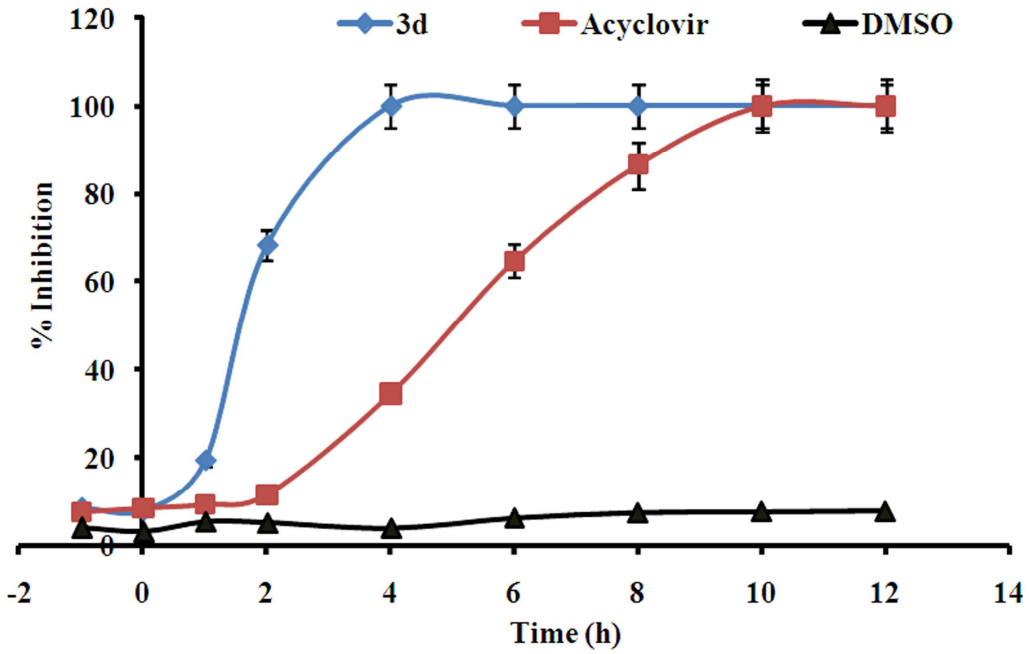

Figure 4 Time of addition assay of **3d** and acyclovir against HSV-1F.

2.2.4 Attachment and penetration assay

The time of addition assay revealed that HSV-1F was inhibited by **3d** at 4-6 hpi which indicates that the action was during early event of viral life cycle including attachment and penetration. Therefore, we investigated these steps separately. The result of attachment and penetration assays showed that **3d** had no effect either on viral attachment or penetration into Vero cells (**Figure 5**) like acyclovir, indicating that **3d** was not inhibiting viral entry to the host cell.

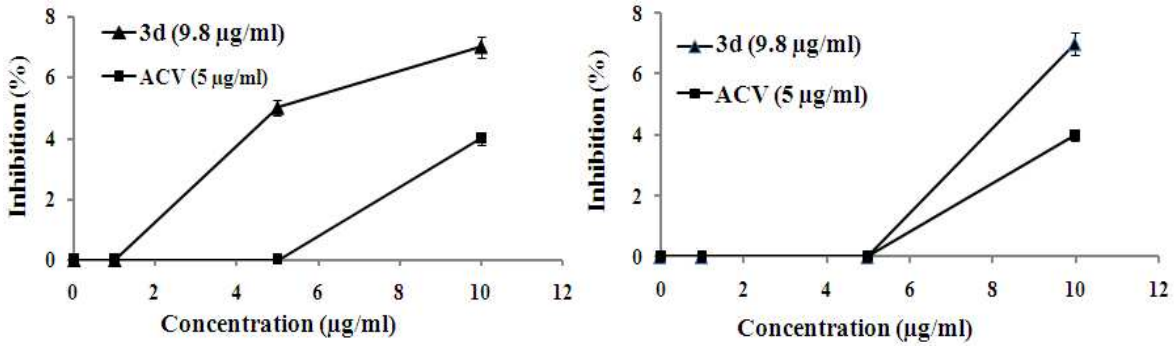

Figure 5 Effect of **3d** and Acyclovir on HSV-1F attachment and penetration respectively.

2.2.5 Drug combination assay

We then examined whether the efficacy of **3d** could be increased in combination with ACV by the drug combination assay. For this we evaluated the antiviral activity of various combinations of **3d** and ACV, alone and in combination, using the isobologram method and assessed by the fractional inhibitory concentration (FIC) index, which represents the sum of the FICs of each drug tested. The FIC for each drug was determined by dividing the MIC of each drug in combination by the MIC of each drug used alone. Based on the Loewe additivity zero-interaction theory a drug cannot interact with itself and the effect of a combination will be additive when FIC index is 1.0. An FIC index smaller or higher than 1 indicates synergy or antagonism.[11-13] Our results showed that FIC index in combination of **3d** and acyclovir was 0.389, indicative of strong synergism (**Table 2**), as found with amphotericin B or voriconazole plus caspofungin (FIC indices 0.5-1.0) that prolonged the survival with reduced fungal burden in aspergillosis;[11] as well as with trifluorothymidine and ganciclovir against HSV-1 at concentrations less toxic than these antivirals alone.[14] Interestingly a minor synergy can augmented the pharmacokinetic and other factors *in vivo.*[15]

Table 2 Inhibitory effects of **3d** in combination with Acyclovir[a]

Compound	EC_{50}	$FIC_{compound} + FIC_{ACV}$	Inhibitory effect
	HSV-1F	HSV-1F	
3d alone	9.8 ± 0.1	-	-
Acyclovir alone	2.4 ± 0.1	-	-
Acyclovir + **3d**	0.75 ± 0.1	0.75/9.8 + 0.75/2.4 = **0.389**	Synergism

[a]The interaction between **3d** and ACV was interpreted according to the combined FIC index [$FIC_{compound} + FIC_{ACV}$] as synergy (≤0.5), no interaction (0.5 - 4) or antagonism (>4) (32).

2.2.6 Effect of compound 3d on HSV early gene expression

It is known that five infected cell proteins (ICPs) ICP0, ICP4, ICP22, ICP27, and ICP47 are the products of immediate early (IE) gene, essential to support the lytic infection of HSV.[16] Among these, ICP4 (product of RS1 gene) is required for the subsequent expression of both early (E) and late (L) viral genes.[17] This protein probably interacts with the basal transcription factors (a part of the RNA polymerase transcription complex) and transactivates the viral gene transcription.[18] On the other hand, the ICP27, encoded by UL54 plays an essential role in viral replication[17] by suppressing host mRNA synthesis through repression of

primary transcription[19] and pre-mRNA splicing.[20] Therefore, to determine the effect of **3d** on HSV early gene expression we measured two essential IE proteins ICP4 and ICP27 by quantitative real-time PCR. The results demonstrated a significant decrease in both IE proteins ICP4 and ICP27 (**Figure 6**) at 2-6 hpi in **3d** treated cells (18 µg/ml), while both were expressed in untreated HSV-1F infected cells.

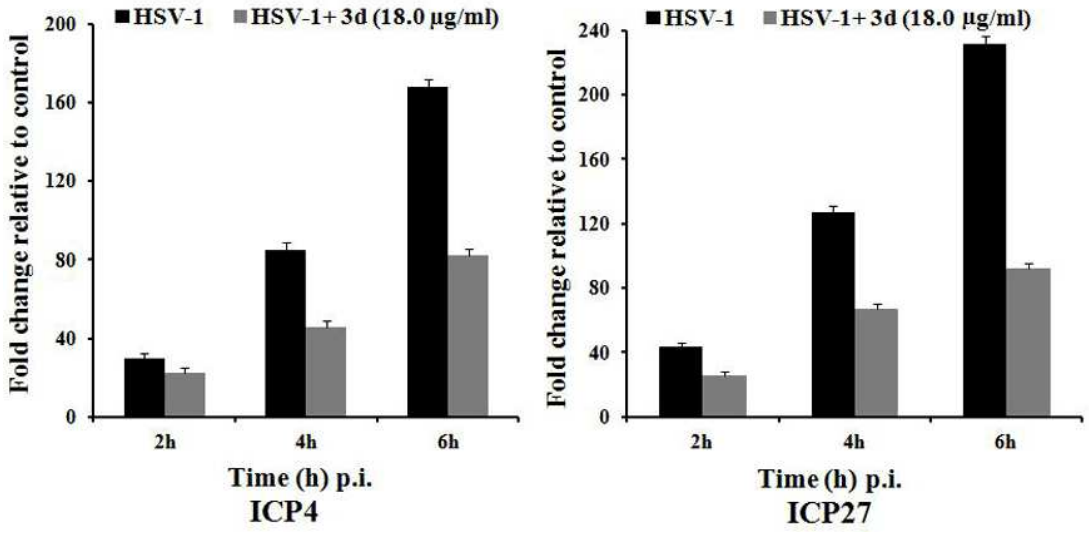

Figure 6 Effect of **3d** on IE gene expression of HSV-1F by Quantitative real time PCR.

2.2.7 Effect of 3d on DNA polymerase expression of HSV-1F

Further, it is known that the DNA polymerase of HSV is encoded by *UL30* gene[21] and exists as a heterodimer in association with UL42 phosphoprotein.[22,23] Moreover, the DNA polymerase is tethered to DNA by the double-strand DNA binding activity of the UL42 protein.[24,25] Therefore, we monitored the expression of viral DNA polymerase in HSV-1F infected cells as well as infected cells treated with the test compound, by immunoblotting. The whole cell extract from HSV-1F infected Vero cells treated with **3d** (9.8 and 18 µg/ml) at 12 hpi was processed for the detection of DNA polymerase. The result (**Figure 7**) demonstrated depletion in HSV DNA polymerase expression level in presence of **3d** compared to the house keeping gene β-actin, indicates **3d** interferes with the HSV DNA polymerase expression.

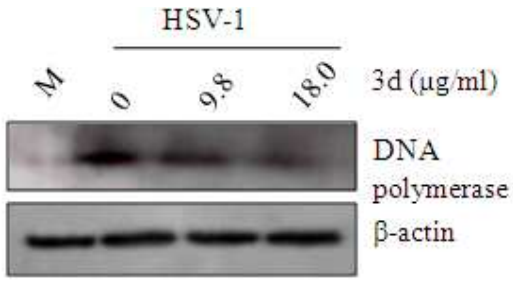

Figure 7 Effect of **3d** on IE gene expression by Western blot analysis.

2.3 Molecular Modeling Studies

In our previous report, we suggested that the binding cleft for pyranone class of molecules may be positioned in the palm sub-domain of HSV DNA polymerase (**Figure 8a**).[3] When the preliminary lead compound (**II)** was docked into the active site, cavity A was partially occupied by the ethanol motif and the cavity B was fully occupied by piperidine motif (**Figure 8b**).

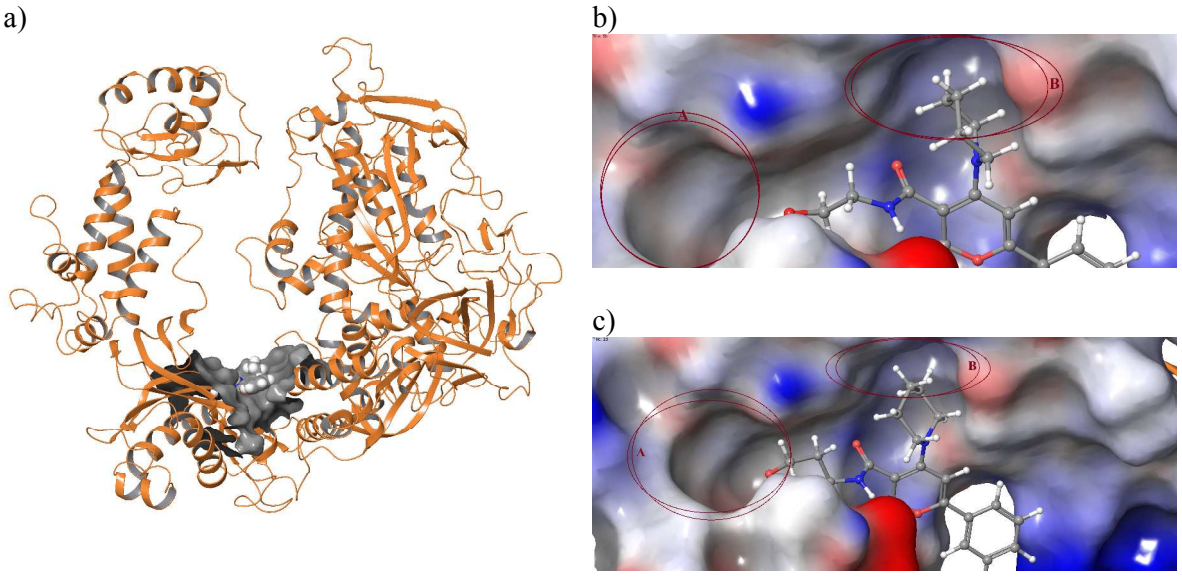

Figure: 8. a) Binding cleft for pyranone class of molecules (shown as black surface) in the palm region of HSV DNA polymerase active site. b) Surface diagram for binding of **II** into the palm region using cavity A and B. c) The surface diagram showing electrostatic surface of the receptor for the binding of **3d** into the palm region using cavity A and B.

Thus in the present manuscript, the cavity A was explored by prototypes **III** in which the ethanol motif was replaced with a propanol motif. The surface diagram for one of the

prototypes (**3d**, **Figure 8c**) reveals similar binding mode as **II** inside the palm region. However, the propanol motif occupied more space in the cavity A. The binding scores of **II** and prototypes **III** summarized in **Table 3** indicate increase in overall binding affinity of **3d** compared **II** which may be the possible reason for enhanced activity. Thus, the present study supports lead optimization to enhance the anti-HSV activity using structure-based approach.

Table 3 The molecular docking studies and scoring for synthesized analogs

	Docking		MM-GBSA Score[c]
Comp	G-Score[a]	Emodel[b]	DG Bind
3a	-4.8	-64.9	-59.9
3b	-6.1	-63.8	-68.4
3c	-5.6	-62.1	-69.5
3d	**-5.7**	**-67.1**	**-72.3**
3e	-5.6	-69.1	-73.1
3f	-5.1	-61.6	-76.8
3g	-5.2	-60.7	-62.3
3h	-5.6	-65.4	-60.7
3i	-5.1	-63.6	-60.7
II	-4.9	-64.9	-68.7

[a]G-Score (Glide Score): The minimized poses are rescored using Schrödinger's proprietary Glide Score scoring function to get G-Score.
[b]Emodel score: The binding affinity can be estimated by Glide Emodel Score, which is the combination of G-Score and non-bonded interaction energy.
[c]MM-GBSA score: Ligand binding energies calculated for all compounds with a single receptor using protein flexibility option (defined: 7 Å from docked ligand). Solvation model: VSGB, The binding energy is calculated according to the equation: DG bind = E_complex (minimized) - E_ligand (minimized) -E_receptor (minimized)

3. Materials and Methods

3.1 Chemistry

3.1.1 General All reactions were carried out in oven-dried glassware under nitrogen atmosphere. The chemicals and solvents were purchased from Spectrochem, Across, Rankem or Sigma-Aldrich. Melting points were recorded on Veego melting point apparatus. Analytical thin layer chromatography (TLC) was performed on precoated plates (silica gel 60 F-254) purchased from Merck Inc. Purification by gravity column chromatography was carried out on silica gel (100-200 mesh). Elico UV/Vis spectrophotometer was used for recording the UV spectra. $^{1}H/^{13}C$ NMR were obtained from a Varian (400 MHz) spectrometer or Bruker spectrometer using $CDCl_3$ or DMSO-d6, as solvents. Peaks are recorded with the

following abbreviations: s, singlet; bs, broad singlet; d, doublet; t, triplet; q, quartet; m, multiplet; *J*, coupling constant (hertz).

3.1.2 Method for synthesis of 2a-c

To a solution of appropriate 2*H*-pyran-4-methylthio-3-carboxylic acid (**1a-c**, 2 mmol) in 15 ml DMF, HATU (2.1 mmol) and diisopropylethylamine (8 mmol) was added and stirred for 15 min. Propanolamine (2.1 mmol) was added and stirred for 5 h at room temperature. The reaction was monitored by TLC for completion. The reaction mixture was poured onto ice water with stirring. The organic layer was separated and the water layer was extracted with DCM. The combined organic layer was dried over anhydrous Na_2SO_4 and concentrated under reduced pressure. The residue was recrystallized with methanol which was used for next reaction.

3.1.3 Method for synthesis of 3a–i

To a solution of an appropriate **2a-c** (1 mmol) in dioxane, appropriate amine (1.5 mmol) was added and refluxed for 6 h and monitored by TLC for completion. The solvent was removed under vacuum; ice cold water was added and extracted with DCM. The organic layer was dried over Na_2SO_4, concentrated under reduced pressure and column purified with 1% methanol in DCM to obtain pure compound.

N-(3-hydroxypropyl)-2-oxo-6-phenyl-4-(pyrrolidin-1-yl)-2*H*-pyran-3-carboxamide (3a)
Yield 55%, mp: 144-145 °C, MS-ESI (m/z): 342.9 [M^++1]; IR (KBr) (ν, cm^{-1}): 3360.00 (NH), 3290 (OH), 1655 and 1624 (C=O); ^{1}H NMR (400 MHz, DMSO-d_6): δ 1.59-1.62 (t, *J* = 6.8 Hz, 2H), 1.88 (s, 4H), 3.18-3.21(t, *J* = 6.8 Hz, 2H), 3.44-3.47 (t, *J* = 6 Hz, 2H), 3.53 (s, 4H), 4.41-4.44 (t, *J* = 5.2 Hz, 1H), 6.79 (s, 1H), 7.51-7.53 (m, 3H),7.89-7.90 (m, 2H), 8.06-8.09 (t, *J* = 5.6 Hz,1H)

6-(4-fluorophenyl)-N-(3-hydroxypropyl)-2-oxo-4-(pyrrolidin-1-yl)-2*H*-pyran-3-carboxamide (3b)
Yield 52%, mp: 188-189 °C, MS-ESI (m/z): 360.9 [M^++1]; IR (KBr) (ν, cm^{-1}): 3365 (NH), 3333 (OH), 1670 and 1639 (C=O); ^{1}H NMR (400 MHz, DMSO-d_6): δ 1.59-1.62 (t, *J* = 6.8 Hz, 2H), 1.88 (brs, 2H), 3.19-3.22 (t, *J* = 6.4 Hz, 2H), 3.43-3.48 (q, *J* = 6 Hz, 2H), 3.52 (brs, 4H), 4.41-4.44 (t, *J* =5.2 Hz, 1H, OH), 6.78 (s,1H),7.34-7.38 (t, *J* = 8.8 Hz, 2H),7.95-7.99 (m, 2H), 8.05-8.08 (t, *J* = 6Hz, 1H, NH).

N-(3-hydroxypropyl)-2-oxo-4-(pyrrolidin-1-yl)-6-(p-tolyl)-2*H*-pyran-3-carboxamide (3c)
Yield 55%, mp: 135-136 °C, MS-ESI (m/z): 357.1 [M^++1]; IR (KBr) (ν, cm^{-1}): 3362 (NH), 3298 (OH), 1661 and 1628 (C=O); ^{1}H NMR (400 MHz, DMSO-d_6): δ 1.59-1.62(t, *J*= 6.4 Hz, 2H), 1.87 (s, 4H), 2.36 (s,3H), 3.17-3.21(t, *J*= 6.4 Hz, 2H), 3.45-3.48 (t, *J*= 6 Hz, 2H), 3.52 (s, 4H), 4.40-4.42 (t, *J*= 5.6 Hz,1H, OH), 6.73 (s,1H), 7.31-7.33 (d, *J*= 8 Hz, 2H), 7.78-7.80 (d, *J* = 8.4 Hz, 2H), 8.02-8.05 (t, *J*=5.6 Hz,1H, NH).

N-(3-hydroxypropyl)-2-oxo-6-phenyl-4-(piperidin-1-yl)-2*H*-pyran-3-carboxamide (3d)
Yield 59%, mp: 172-173 °C, MS-ESI (m/z): 356.9 [M^++1]; IR (KBr) (ν, cm^{-1}): 3362 (NH), 3289 (OH), 1656 and 1627 (C=O); ^{1}H NMR (400 MHz, DMSO-d_6): δ 1.59-1.62 (m, 8H), 3.18-3.23 (t, *J* =6.8 Hz, 2H), 3.39-3.46 (m,6H), 4.42-4.45 (t, *J*= 5.2 Hz, 1H, OH), 6.98 (s,1H), 7.51-7.52 (t, *J* = 3.2 Hz, 3H), 7.91-7.92 (d, *J* =2.8 Hz, 2H), 8.15 (s,1H, NH).

6-(4-fluorophenyl)-N-(3-hydroxypropyl)-2-oxo-4-(piperidin-1-yl)-2*H*-pyran-3-carboxamide (3e)
Yield 54%, mp: 166-167 °C, MS-ESI (m/z): 374.9 [M^++1]; IR (KBr) (ν, cm^{-1}): 3367 (NH), 3306 (OH), 1666 and 1628 (C=O); ^{1}H NMR (400 MHz, DMSO-d_6): δ 1.59-1.62 (m, 8H), 3.18-3.23 (q, *J* = 6.8 Hz, 2H), 3.43-3.47 (m, 6H), 4.42-4.45 (t, *J* = 5.2 Hz, 1H, OH), 6.97 (s, 1H), 7.34-7.38 (t, *J* =8.8 Hz, 2H), 7.98-8.02 (m, 2H), 8.13-8.16 (t, *J* =5.6 Hz, 1H, NH).

N-(3-hydroxypropyl)-2-oxo-4-(piperidin-1-yl)-6-(p-tolyl)-2*H*-pyran-3-carboxamide (3f)
Yield 55%, mp: 153-154 °C, MS-ESI (m/z): 371.1 [M^++1].; IR (KBr) (ν, cm^{-1}): 3359 (NH), 3292 (OH), 1661 and 1631 (C=O); ^{1}H NMR (400 MHz, DMSO-d_6): δ 1.59-1.64 (m, 8H), 2.37 (s, 3H), 3.18-3.21 (t, *J*= 6.4 Hz, 2H), 3.43-3.47 (m, 6H), 4.41-4.43 (t, *J*= 5.6 Hz,1H, OH), 6.92 (s,1H), 7.31-7.33 (d, *J*=8 Hz, 2H), 7.81-7.83 (d, *J*=8.4 Hz, 2H), 8.12-8.15 (t, *J*=5.6 Hz,1H, NH).

4-(dimethylamino)-N-(3-hydroxypropyl)-2-oxo-6-phenyl-2*H*-pyran-3-carboxamide (3g)
Yield 45%, mp: 132-133 °C, MS-ESI (m/z): 316.9 [M^++1]; IR (KBr) (ν, cm^{-1}): 3359 (NH), 3286 (OH), 1654 and 1630 (C=O); ^{1}H NMR (400 MHz, DMSO-d_6): δ 1.61-1.64 (t *J* = 6.4 Hz, 2H), 3.10 (s,6H), 3.19-3.24 (q, *J* = 6 Hz, 2H), 3.43-3.48 (q, *J* =5.6 Hz, 2H), 4.42-4.45(t, *J* = 5.2 Hz, 1H, OH), 6.91(s,1H), 7.47-7.53 (m, 3H), 7.90-7.93 (m, 2H), 8.09-8.12 (t, *J* =5.6 Hz,1H, NH).

4-(dimethylamino)-6-(4-fluorophenyl)-N-(3-hydroxypropyl)-2-oxo-2*H*-pyran-3-carboxamide (3h)
Yield 42%, mp: 112-113 °C, MS-ESI (m/z): 335.2 [M^++1]; IR (KBr) (ν, cm^{-1}): 3361 (NH), 3309 (OH), 1649 and 1624 (C=O); ^{1}H NMR (400 MHz, DMSO-d_6): δ 1.57-1.60 (t, *J* = 6.4 Hz, 2H), 3.12 (s, 6H), 3.18-3.23 (q, *J* =6.8 Hz, 2H), 3.46-3.49 (t, *J* = 6.4 Hz, 2H), 4.46-4.49 (t, *J* =5.2 Hz, 1H, OH), 6.89 (s,1H), 7.31-7.34 (t, *J* =8.6 Hz, 2H), 8.01-8.13 (m, 2H), 8.15-8.18 (t, *J* =5.6 Hz,1H, NH).

4-(dimethylamino)-N-(3-hydroxypropyl)-2-oxo-6-(p-tolyl)-2*H*-pyran-3-carboxamide (3i)
Yield 45%, mp: 86-87 °C, MS-ESI (m/z): 331.1 [M^++1]; IR(KBr) (ν, cm^{-1}): 3355 (NH), 3291(OH), 1651 and 1632 (C=O); ^{1}H NMR (400 MHz, DMSO-d_6): δ 1.57-1.64 (m, 2H), 2.49 (s,3H), 3.09 (s, 6H), 3.19-3.22 (q, *J* =6.4 Hz, 2H), 3.43-3.48 (q, *J* = 6.4 Hz, 2H), 4.31-4.44 (t, *J* =5.2 Hz,1H,OH), 6.85 (s,1H), 7.32-7.34 (d, *J* =8.3 Hz, 2H), 7.80-7.82 (d, *J* =8Hz, 2H), 8.07-8.10 (t, *J* =5.2 Hz,1H, NH).

3.2 Biological Evaluations

3.2.1 *Cell and viruses*:

Vero cells (African green monkey kidney cells; ATCC, Manassas, VA, USA) were cultured in Dulbecco's modified Eagle's medium (DMEM) with 5-10% fetal bovine serum (FBS;

Invitrogen, USA), 100 U/mL penicillin and 100 µg/mL streptomycin, at 37ºC in 5% CO_2. The viral strains used were HSV-1F and HSV-2G (ATCC 734), purchased from the ATCC (Manassas, VA, USA). Virus stocks were prepared from infected culture at a multiplicity of infection (moi) of 0.5 for 1 h at 37ºC. The residual viruses were then washed out with phosphate-buffered saline (PBS) and the cells were cultured for another 48-72 h. The cultured cells were lysed finally by three cycles of freezing and thawing, centrifuged at 1500 *g* at 4ºC for 20 min and the collected supernatant was tittered by plaque assay, and stored at -80ºC for further studies.

3.2.2 ***Cytotoxicity assay***:

To determine the effect of the test compounds on uninfected cells, cultured Vero cells (10^4 cells/well) in 96 well plates were exposed to various concentrations of the test drugs, in triplicate and incubated at 37ºC in 5% CO_2, using ACV and dimethylsulfoxide (DMSO, 0.1%) as controls. After 48 h, 10% 3-(4,5-dimethylthiazol-2-yl)-2,5-diphenyl tetrazolium bromide (MTT; Sigma) was added to each well with DMEM, incubated for 3-4 h, and then mixed with 100 µl of MTT solubilising solution (Sigma), and the optical density (OD) was read by a plate reader at 570 nm with a reference wavelength of 690 nm. Data were calculated as the percentage of cell viability using the formula: [(sample absorbance-cell free sample blank)/mean media control absorbance)] X100%. The 50% cytotoxic concentration (CC_{50}) causing visible morphological changes in 50% of Vero cells with respect to cell control was determined from the concentration-response curves after viable cell count.[9, 26]

3.2.3 ***Antiviral activity by Plaque reduction assay***:

Plaque reduction assay was used to evaluate the antiviral efficacy of the test compound(s), using ACV and DMSO (0.1%) as positive and negative control respectively. Vero cell monolayer in six well plates, infected with HSV-1F and HSV-2G (100 pfu) were exposed to serial dilutions of test compound for 1-2 h at 37ºC, then washed with PBS and overlaid with 1% methylcellulose (Fluka, USA) to form plaques. The plaques developed after 72 h of incubation were fixed with 4% paraformaldehyde and stained with methylene blue (0.03%) in 70% methanol. The virus titers were calculated by scoring the plaque-forming units (pfu). The effective concentration of test compound that inhibited the number of viral plaques by 50% (EC_{50}) was interpolated from the dose-response curves.[27-29]

3.2.4 ***Dose response assay***

The Vero cell (10^4 cells/well) culture on 96-well plates were infected with HSV-1F and HSV-2G (1 moi) separately and then exposed to various concentrations of test compounds (0-50 µg/ml) and ACV, in triplicate, and incubated for 72 h at 37ºC in 5% CO_2. The MTT assay was carried out, as described above and viral inhibition rate was calculated as: $[(A_{tv}-A_{cv})/(A_{cd}-A_{cv})]X100\%$, where A_{tv} indicates the absorbance of test compound with virus-infected cells. A_{cv} indicates the absorbance of virus control, and A_{cd} the absorbance of the cell control. The antiviral concentration of 50% effectiveness (EC_{50}) was defined as the concentration that achieved 50% inhibition of virus-induced cytopathic effects.[30]

3.2.5 *Time response assay*:

Following three different approaches, Vero cells were exposed to the test compound (18.0 µg/ml) before infection, during infection or after infection with HSV-1F (100 pfu/well) at 0-12 h time intervals in triplicate, using DMSO (0.1%) and ACV (5.0 µg/ml) as controls. For pre-infection Vero cells were treated with the test compound either for 1 h or for 3 h, washed with PBS and then infected with the virus in DMEM containing 2% FBS at 37°C. For co-infection cells were subsequently infected and treated with the test compound and after 1 h of incubation the virus-drug mixture was removed, washed with PBS three times, and added with fresh media. While for post-infection (p.i) the cells were infected with HSV-1F first, allow adsorbing (1 h) and then treated with the test compound. Then the mixture was removed from the respective well(s) at different time intervals upto 12 h, washed with PBS and added with the fresh media to carry out the plaque reduction assay, as described above.[27-29, 31]

3.2.6 *Attachment and penetration assay*:

To investigate whether the compound have any effect on viral adsorption or attachment, Vero cell monolayer were prechilled at 4ºC for 1 h and subsequently challenged with HSV-1F (200 pfu/well) in the presence of test compound (9.8 µg/ml), DMSO (0.1%) or ACV (5.0 µg/ml) for 3 h at 4ºC. After infection, the wells were washed twice with ice-cold PBS to remove unbound virus, and overlaid with 1% methylcellulose to allow plaque formation. The plaques developed after 72 h of incubation were stained and counted.[32]

For viral penetration assay prechilled (at 4°C for 1 h) Vero cell monolayer were subsequently incubated with HSV-1F (300 pfu/well) for 3 h at 4°C to allow viral adsorption. The infected cells were then incubated with test compound (18.0 µg/ml), DMSO (0.1%) or ACV (5.0

µg/ml) for another 20 min at 37°C to facilitate viral penetration. At the end of the incubation period, extracellular non-penetrated virus was inactivated by citrate buffer (pH 3.0) for 1 min, and then the cells were washed with PBS and overlaid with overlay medium for plaque formation. The viral plaques developed after 48 h of incubation at 37ºC were stained and counted.[32]

3.2.7 *Combined effect of test compound with Acyclovir*

In order to analyze the combined effect of test compound (3d) and ACV on plaque formation the EC_{50} of these agents at various concentrations of the compounds against HSV-1F were tested. The combined effect of both the agents on HSV was examined by plaque assay. Duplicate culture of Vero cells were infected with 100 PFU/0.2 ml of HSV-1F for 1 h and the cells were overlaid with 5 ml of overlay medium containing 1% methylcellulose with various concentrations of the test compound and/or ACV and then incubated at 37 ºC for 5 days. The cells were washed and then fixed (4% paraformaldehyde) and stained with methylene blue (0.03%) to count the numbers of plaques for the determination of 50% inhibitory concentration of the plaque number from a curve, while the combined treatment was analyzed by isobologram method.[12,15,33] The EC_{50} was used to calculate the fractional inhibitory concentration (FIC) of the agents in combination[9]. The interaction between test compound and ACV was interpreted according to the combined FIC index ($FIC_{compound} + FIC_{ACV}$) as synergy (≤0.5), no interaction (0.5-4) or antagonism (>4).[15,33]

3.2.8 *Quantitative real-time PCR:*

HSV-1F (5 moi) infected Vero cells were treated with the test compound (9.8 and 18.0 µg/ml) for 2 h, 4 h and 6 h post-infection and immediately, RNA was isolated using RNeasy Mini kit (QIAGEN) following the manufacturer's protocol. Total RNA (0.1 mg/ml) in RNase-free water in 20 µl of RT mix (containing 5X VILO Reaction Mix, 10X SuperScript Enzyme Mix and DEPC treated water) was subjected to cDNA synthesis using the GeneAmp PCR System 9600 (Perkin Elmer Corp, USA). Then real-time PCR was performed with these products by using SYBR Green PCR Master Mix (Qiagen) following manufacturer protocol in a ABI Prism 7000 sequence detection system (Applied Biosystems, CA, USA). The PCRs were amplified at cycling conditions of: 95ºC for 10 min and 40 cycles (15 s at 95°C, then 60 s at 60°C) in triplicate.[34,35] The sequences of primers used were as follows: ICP4 (5'-GACGTTGTGGACTGGGAAG-3' and 5'-ACTTAATCAGGTCGTTGCCG-3'); ICP27 (5'-CCTTTCTCCAGTGCTACCTG-3' and 5'-GCCAGAATGACAAACACGAAG-3') and

GAPDH (5'-AAGGTCGGAGTCAACGGATT-3' and 5'-CTGGAAGATGGTGATGATGGGATT-3').

3.2.9 *Western blot analysis of DNA polymerase:*

For Western blot analysis, equal amounts of protein (40 µg/sample) from HSV-1F infected and untreated or treated cells with test compound (9.8 and 18.0 µg/ml) at 12 h p.i. for HSV DNA polymerase were immediately harvested in buffer (200 µl per well) containing 20 mM Tris (pH 7±0.5), 50 mM NaCl, 5% NP-40, 0.05% DOC and separated by centrifugation at 16000 g with a microcentrifuge for 10 min at 4°C, subjected to SDS-PAGE and blotted to pre-equilibrated PVDF membrane (Thermo scientific, USA). Then the membrane was blocked in 5% NFDM in 1X TBST (20 mM Tris, pH 7.5, 150 mM NaCl, 0.5% Tween 20), rinsed and incubated with anti- HSV DNA polymerase or polyclonal anti-β-actin (Shanta Cruz Biotech Inc., USA) antibody in 5% BSA at 4°C overnight. Immunoblotting was performed with peroxidase-labeled anti-rabbit polyclonal antibodies and visualized by ECL Western blotting detection kit (Millipore, USA).[34,35]

3.3 Molecular Modeling

3.3.1 Receptor preparation

In continuation to our modeling studies, the previously prepared and reported structure of HSV DNA polymerase was used[9] and optimized by protein preparation wizard (PPW) of Schrödinger Suite 2013.[36]

3.3.2 Ligands preparation

The 3D structure for synthesized compounds were built using Maestro interface of Schrödinger. The hydrogens were added, valances were satisfied, all bonds were corrected and formal charges were assigned. Finally all compounds were treated in LigPrep module[37] of Schrödinger using OPLS force field 2005 followed by conformational search through MacroModel MMFFs force field to obtained the suitable conformations. The lowest energy conformer was selected for each compound to perform molecular docking studies. The reference compound **II** has been used as primary lead and prepared for docking studies.

3.3.3 Molecular docking

The receptor grid generation and molecular docking studies were conducted by Glide module[37-38] of Schrodinger Suite 2013. The grid was generated around the catalytic traid of

aspartic acid residues (717, 886 and 888) which has been reported essential for the polymerase activity in HSV DNA-polymerase. Glide module of Schrodinger suite 2013 was used to perform docking analysis. All ligand compounds including reference compound **II** were docked at the predefined receptor grid using extra precision mode (XP)[40] mode.

3.3.4. Embrace minimization

The top score (G-score, Table 3) docked pose of each compounds were subjected to eMBrAcE module of MacroModel[41] for simulation to determine the binding energy differences. The minimization was performed using OPLS2005 force field utilizing GB/SA continuum water solvation model. During eMBrAcE minimization, all the residues were allowed to move freely. Minimization was conducted for 5000 steps or until the energy difference between subsequent conformations attains 0.05 kJ/mol. The energy difference results were obatined based on the calculation using $\Delta E = E_{complex} - (E_{ligand} + E_{protein})$.

3.3.5 Ligand free energy of binding energy calculation

The best two docked structures obtained after Glide docking were compared by minimizing with local optimization in Prime and the energies of the complex were calculated using OPLS 2005 force field and Generalized-Born/Surface Area continuum solvent model. The Prime MMGBSA was used to calculate the binding free energy DG of ligands. Using equation $DG = \Delta E_{MM} + \Delta Gsolv + \Delta GSA$, where ΔEMM is the difference between the minimized energy of the Ligand-HSVcomplex and the sum of the minimized energies of HSV protein and ligands. ΔGSA is the difference in surface area energies for the complex and the sum of the surface area energies for the individual molecules .ΔGsolv is the difference in the generalized-Born/surface area

4. Summary and Conclusions

The present study reveals the structure based optimization of preliminary lead compound **II** to a potential lead candidate **3d** as possible anti-HSV agent. A modeling study suggests that **3d** can effeciently utilized tubular cavity-A for binding with HSV DNA polymerase and opens a future scope for drug candidate development. The newly synthesized compound **3d** demonstrated the promissing anti-HSV activity and biological studies were conducted to understand possible mode of action. The MTT and plaque reduction assay revealed that **3d**

has moderate antiviral activity against HSV-1F and HSV-2G with respect to its EC_{50} and selectivity index, compared to ACV. The plaque reduction assay demonstrated that **3d** inhibited HSV-1F and HSV-2G infection in a dose-dependent manner and >99% inhibition was achieved at 18.0 and 24.0 μg/ml. In order to understand the quantitative and temporal aspects of the antiviral activity of **3d**, we conducted kinetic studies, which revealed that the addition of **3d** to virus infected cells at 4-6 h post-infection is highly effective in killing the virus. Further study showed that **3d** was unable to prevent the attachment or penetration of HSV, like ACV, suggesting that the mode of action of **3d** is not the prevention of viral adsorption or penetration, but perhaps the interference of early events of HSV replication. Moreover, the drug combination assay (**3d** ± ACV) showed strong synergistic effects, suggesting that **3d** may work through similar targets but at different time points. Next, to investigate the possible mode of action of **3d** on early events of viral infection cycle we studied the effect of **3d** on IE gene expression of HSV. To study whether **3d** interferes any of the events of IE gene expression first we measure the two major end products, ICP4 and ICP27 of IE gene by quantitative real-time PCR analysis. The results demonstrated the reduced expression of both ICP4 and ICP27 in HSV infected **3d** treated cells but not in untreated cells. Furthermore, the depletion of viral DNA polymerase expression, demonstrated by immunoblotting studies, in HSV-1F infected cells treated with **3d** indicated that it can prevent HSV multiplication.

Acknowledgements
This research received funding from Department of Biotechnology (DBT), Delhi, India through grant no BT/PR14237/MED/29/196/2010 and BT/PR13759/PBD/17/686/2010. SK thanks CSIR, India for Senior Research Fellowships (SRF). Authors acknowledge Cosmic Discoveries Ltd. ILS, Hyderabad for NMR-Mass Facility, and Central Instrument Facility, BIT Mesra for analytical support.

References

1. A. J. Phillips, *J. Biomed. Inform.*, 2006, **39**, 18-33.
2. R. J. Brideau, M. L. Knechtel, A. Huang, V. A. Vaillancourt, E. E. Vera, N. L. Oien, T. A. Hopkins, J. L. Wieber, K. F. Wilkinson and B. D. Rush, *Antiviral Res.*, 2002, **54**, 19-28.
3. N. L. Oien, R. J. Brideau, T. A. Hopkins, J. L. Wieber, M. L. Knechtel, J. A. Shelly, R. A. Anstadt, P. A. Wells, R. A. Poorman and A. Huang, *Antimicrob Agents Chemother***.**, 2002, **46**, 724-730.
4. J. Piret, G. Boivin, G. *Antimicrob. Agents Chemother*. 2011, **55**(2), 459-472.

5. M.N. Prichard, E.R. Kern, C.B. Hartline, E.R. Lanier, D.C. Quenelle. *Antimicrob Agents Chemother*. 2011, **55**(10), 4728-4734.
6. J.L. Coleman, D. Shukla. *Vaccin Immunother*. 2013, **9**(4), 729-735.
7. C. Johnston, D.M. Koelle, A. Wald. *J. Clin. Investig*. 2011, **121**(12), 4600-4609.
8. K. Modjarrad, S.H. Vermund. *Lancet Infect Dis*. 2010, **10**(7), 455-463.
9. S. Karampuri, P. Bag, S. Yasmin, D. K. Chouhan, C. Bal, D. Mitra, D. Chattopadhyay and A. Sharon, *Bioorg. Med. Chem. Lett.*, 2012, **22**, 6261-6266.
10. $C_{20}H_{24}N_2O_4$, M = 356.4, triclinic, space group: P-1, a = 8.0084 (5), b = 11.0499 (7), c = 11.0645 (7) Å, a = 70.326 (5), b = 80.844 (5), g = 71.336 (6), V = 872.03 (10) Å3, T = 99.9 (2) K, Z = 2, m = 0.31 mm-1, F(000) = 377.4, Dc = 1.353 Mg m-1, yellow rectangular crystal, crystal size: 0.20 x 0.26 x 0.11 mm, 4704 reflections measured, 3038 unique, R1 =0.0438 for 2605 Fo > 4sig(Fo) and 0.0509 for all 3038 data and 312 parameters with Goodness of fit GooF = 1.079. Unit cell determination and intensity data collection (2θ range = 8-133.2°) was performed with 99.8% completeness at 99.9 (2) K. Structure solutions by direct methods and refinements by full-matrix least-squares methods on F2. CCDC 970219 contains the supplementary crystallographic data for this paper. These data can be obtained from The Cambridge Crystallographic Data Centre via www.ccdc.cam.ac.uk/data_request/cif.
11. J. Meletiadis, S. Pournaras, E. Roilides, and T.J. Walsh. *Antimicrob Agents Chemother*., 2010, **54**(2), 602-609.
12. V. Petraitis, R. Petraitiene, W. W. Hope, J. Meletiadis, D. Mickiene, J. E. Hughes, M. P. Cotton, T. Stergiopoulou, M. Kasai, A. Francesconi, R. L. Schaufele, T. Sein, N. A. Avila, J. Bacher, T. J. Walsh *Antimicrob Agents Chemother*., 2009, **53**, 2382-2391.
13. M. C. Berenbaum. *Pharmacol Rev*., 1989, **41**, 93-141.
14. J.A. Hobden, M. Kumar, H.E. Kaufman, C. Clement, E.D. Varnell, P.S. Bhattacharjee, J. M. Hill. *Invest Ophthalmol Vis Sci*., 2011, **52**(2), 830-833.
15. M. C. Berenbaum**.** *J. Antimicrob. Chemother*., 1987, **19**, 271-273.
16. R. W. Honess and B. Roizman, *Proc Natl. Acad. Sci. USA*, 1975, **72**, 1276-1280.
17. J. P. Weir, *Virus Genes*, 1998, **16**, 85-93.
18. C. A. Smith, P. Bates, R. Rivera-Gonzalez, B. Gu and N. A. DeLuca, *J. Virol.*, 1993, **67**, 4676-4687.
19. C. A. Spencer, M. E. Dahmus and S. A. Rice, *J. Virol.*, 1997, **71**, 2031-2040.
20. M. A. Hardwicke and R. M. Sandri-Goldin, *J. Virol.*, 1994, **68**, 4797-4810.
21. J. S. Gibbs, H. C. Chiou, J. D. Hall, D. W. Mount, M. J. Retondo, S. K. Weller and D. M. Coen, *Proc Natl. Acad. Sci. USA*, 1985, **82**, 7969-7973.
22. I. R. Lehman and P. E. Boehmer, *J. Biol. Chem.*, 1999, **274**, 28059-28062.
23. P. J. Vaughan, D. J. Purifoy and K. L. Powell, *J. Virol.*, 1985, **53**, 501-508.
24. M. L. Gallo, D. I. Dorsky, C. S. Crumpacker and D. S. Parris, *J. Virol.*, 1989, **63**, 5023-5029.
25. M. L. Gallo, D. H. Jackwood, M. Murphy, H. S. Marsden and D. S. Parris, *J. Virol.*, 1988, **62**, 2874-2883.
26. Y. Zhang, P. P. But, V. E. Ooi, H. X. Xu, G. D. Delaney, S. H. Lee and S. F. Lee, *Antiviral Res.*, 2007, **75**, 242-249.
27. D. Ojha, H. Mukherjee, S. Ghosh, P. Bag, S. Mondal, N. Chandra, K. Mondal, S. Chakrabarti, A. Samanta, D. Chattopadhyay. *Journal of Applied Microbiology*, 2013, **115**, 1317-1328.
28. P. Bag, D. Chattopadhyay, H. Mukherjee, D. Ojha, N. Mandal, M. C. Sarkar, T. Chatterjee, G. Das and S. Chakraborti, *Virol. J.*, 2012, **9**, 98.

29. D. Chattopadhyay, M. C. Sarkar, T. Chatterjee, R. Sharma Dey, P. Bag, S. Chakraborti and M. T. Khan, *New Biotechnol.*, 2009, **25**, 347-368.
30. H. Y. Cheng, T. C. Lin, C. M. Yang, K. C. Wang, L. T. Lin and C. C. Lin, *J. Antimicrob. Chemother.*, 2004, **53**, 577-583.
31. H. Mukherjee, D. Ojha, P. Bag, H. S. Chandel, S. Bhattacharyya, T. K. Chatterjee, P. K. Mukherjee, S. Chakraborti and D. Chattopadhyay, *Microbiol. Res.*, 2013, **168**, 238-244.
32. L. T. Lin, T. Y. Chen, C. Y. Chung, R. S. Noyce, T. B. Grindley, C. McCormick, T. C. Lin, G. H. Wang, C. C. Lin and C. D. Richardson, *J. Virol.*, 2011, **85**, 4386-4398.
33. J. Piret, S. Roy, M. Gagnon, S. Landry, A. Desormeaux, R. F. Omar and M. G. Bergeron, *Antimicrob. Agents Chemother.*, 2002, **46**, 2933-2942.
34. S. La Frazia, C. Amici and M. G. Santoro, *Antivir. Ther.*, 2006, **11**, 995-1004.
35. P. Bag, D. Ojha, H. Mukherjee, U. C. Halder, S. Mondal, S. Nandi, A. Sharon, S. Chakrabarti, D. Chattopadhyay. *PLoS One*, 2013, **8**(10), e77937.
36. Schr□dinger, Suite 2013, LLC, New York, NY, 2013.
37. *LigPrep-V-2.7*, Schr□dinger, LLC, New York, NY, 2013.
38. *Glide-V-6.0*, Schr□dinger, LLC, New York, NY, 2013.
39. T. A. Halgren, R. B. Murphy, R. A. Friesner, H. S. Beard, L. L. Frye, W. T. Pollard and J. L. Banks, *J. Med. Chem.*, 2004, **47**, 1750-1759.
40. R. A. Friesner, R. B. Murphy, M. P. Repasky, L. L. Frye, J. R. Greenwood, T. A. Halgren, P. C. Sanschagrin and D. T. Mainz, *J. Med. Chem.*, 2006, **49**, 6177-6196.
41. *MacroModel-V-10.1*, Schr□dinger, LLC, New York, NY, 2013.